

Compact and Hexaband Rectangular Microstrip Patch Antenna for Wireless Applications

Revansiddappa S kinagi (✉ revansk@gmail.com)

Visvesvaraya Technological University <https://orcid.org/0000-0002-6680-5851>

RAVI M Yadahalli

Hirasugar Institute of Technology

Siddarama R Patil

PDA College of Engineering: Poojya Doddappa Appa College of Engineering

Research Article

Keywords: Microstrip patch antenna, Hexaband, Compact, Split Ring, C Slot.

Posted Date: March 16th, 2021

DOI: <https://doi.org/10.21203/rs.3.rs-254042/v1>

License: © ⓘ This work is licensed under a Creative Commons Attribution 4.0 International License.

[Read Full License](#)

Compact and Hexaband Rectangular Microstrip Patch Antenna for Wireless Applications

Revansiddappa Kinagi · Ravi M Yadahalli · Siddarama Patil

Received: date / Accepted: date

Abstract

A Compact Corner Split Ring with Split C Slot Rectangular Microstrip patch Antenna (CCSR-SCS) fed by a 50Ω microstripline is discussed. A Corner split ring with C shaped slot has been etched in rectangular microstrip antenna. The slot increases the length of the surface current for the dominant mode TM_{10} leading to the decrease in resonance frequency. The size reduction along with proposed antenna Hexaband is obtained with the antenna and it is best suited for wireless communication. The proposed work is simulated using 3DEM of Mentorgraphics. The results show that Hexaband with compactness is achieved.

Keywords Microstrip patch antenna, Hexaband, Compact, Split Ring, C Slot.

1 Introduction

Since the introduction of wireless networking and portable devices the need for light weight antennas is growing. Because of the low profile and planar

Revansiddappa Kinagi
Department of E & CE, Sharnbasva University Kalaburagi, India
E-mail: revansk@gmail.com

Ravi M Yadahalli
Department of E & CE, Hirasugar Institute of Technology Nidasoshi, Belagavi, India.
E-mail: yadahalliravim@gmail.com

Siddarama Patil
Department of E & CE, PDA College of Engineering Kalaburagi, India.
E-mail: pdapatil@gmail.com

configuration the Rectangular Microstrip Patch Antenna (RMSA) is used widely. Nevertheless, the size of the low frequency RMSA becomes large and the bandwidth is small. Many techniques for obtaining both the compact and broadband antennas were published in the literature, such as high relative permittivity substrates (ϵ_r), shorting pins at appropriate position inside the radiating patch and etched slits etc... [1–5]. Advancements in the wireless communication field involve innovative RMSAs which provide dual or triple band to avoid using two or more antennas and that can also allow size reduction. Mobile telephony systems for example, allow portable devices compliant with GSM900/DCS1800/ UMTS2000 technologies and the same devices will also link users to WLAN networks based on 802.11 standards (2.4/3.6/4.9/5.9GHz) specifications. Hence, it is of great interest to develop patch antenna with multiple resonances [4–7]. Many researchers have made huge efforts to design slot/slit based antennas on the radiating patch and ground plane, which can be used for multiband operations [8–14]. Reconfigurable antennas are still attracting many researchers for designing multiband antennas [15–17]. Metamaterials are the promising new candidates for designing multiband antennas [18–20]. Fractals have been investigated for multiband antenna operations [21, 22]. Stacking of antennas for multiband operation has also been investigated [23, 24].

Effort has been made in this paper to obtain compactness and Hexaband. The Compact Corner Split Ring and Split C Slot Rectangular Microstrip patch Antenna (CCSR-SCS) is simulated using Mentor graphics 3DEM simulation environment and validated using Vector Network Analyzer (VNA).

2 Antenna Design

The design of RMSA is carried out based on transmission line model proposed by Munson First and foremost substrate material is selected. For the selected substrate, the main electrical properties taken into considerations are relative permittivity (ϵ_r) and loss tangent ($\tan \delta$). Substrate with higher relative permittivity results in smaller patch, which reduces impedance bandwidth as well as it results in tighter tolerances towards manufacture. A high loss tangent decreases antenna performance in terms of antenna efficiency and increases feed loss. The substrate thickness (h) is so chosen to be as high as possible in order to maximize impedance bandwidth as well as efficiency but not as high as the chance of excitation of surface waves. Usage of substrate material having higher relative permittivity decreases radiation losses due to much of the Electro-Magnetic field between the radiating patch and the ground is localized in the dielectric. The value of h is selected as per the equation,

$$h \leq \left(\frac{0.3c}{2\pi f_0 \sqrt{\epsilon_r}} \right) \quad (1)$$

Where, c is the speed of light in cm and f_0 is maximum operating frequency in GHz.

Glass epoxy substrate material is one of the low cost and easily available substrate materials commonly used in the printed circuit board (PCB). The

antennas are commonly fabricated using this substrate, for testing the new designs.

A. Design of RMSA

For known values of ϵ_r , h , resonant frequency f_r and λ_0 , the design of RMSA is as follows.

1. Design of elemental width (W) : The elemental width of RMA is

$$W = \frac{c}{2f_r} \sqrt{\frac{2}{\epsilon_r + 1}} \quad (2)$$

2. Design of extension length (Δl):

The extension length Δl is usually deducted from the calculated length L of RMSA in order to retain actual length of the RMSA. The extension length virtually appears due to fringing fields as

$$\Delta l = 0.412h \left(\frac{(\epsilon_e + 0.3) \left(\frac{W}{h} + 0.264 \right)}{(\epsilon_e - 0.258) \left(\frac{W}{h} + 0.8 \right)} \right) \quad (3)$$

Where ϵ_e is the effective dielectric constant. It is calculated by using

$$\epsilon_e = \frac{\epsilon_r + 1}{2} + \frac{\epsilon_r - 1}{2} \left(1 + 12 \frac{h}{W} \right)^{-\frac{1}{2}} \quad (4)$$

3. Design of elemental length (L) :

Once the extension length (Δl) and effective dielectric constant (ϵ_e) are determined using equations (3) and (4) then the elemental length of CRMA is found by using the equation.

$$L = \frac{c}{2f_r \sqrt{\epsilon_e}} - 2\Delta l \quad (5)$$

4. Design of microstripline feed:

The design of 50Ω microstripline feed is carried out by calculating W/h ratio for the known values of characteristic impedance Z_0 and ϵ_r . The design equations are

$$\frac{W_f}{h} = \left(\frac{8e^A}{e^{2A} - 2} \right) \text{ for } \frac{W_f}{h} < 2 \quad (6)$$

$$\frac{W_f}{h} = \frac{2}{\pi} \left[B - 1 - \ln(2B - 1) + \frac{\epsilon_r - 1}{2\epsilon_r} \left\{ \ln(B - 1) + 0.39 - \left(\frac{0.61}{\epsilon_r} \right) \right\} \right] \quad (7)$$

$$\text{for } \frac{W_f}{h} > 2$$

where,

$$A = \frac{Z_0}{60} \sqrt{\frac{\epsilon_r + 1}{2}} + \frac{\epsilon_r - 1}{\epsilon_r + 1} \left(0.23 + \frac{0.11}{\epsilon_r} \right) \quad (8)$$

and

$$B = \frac{377\pi}{2Z_0\sqrt{\epsilon_r}} \quad (9)$$

By using equations (6) to (9) the width of microstripline feed W_f may be determined by multiplying the value of h to the value obtained from equation (6) or (7) as per their. The length $L/4$ for single element RMA in order to keep minimum loss in microstripline feed and is given by

$$L_f = \frac{\lambda_g}{4} \quad (10)$$

$$\lambda_g = \frac{\lambda_o}{\sqrt{\epsilon_{eff}}} \quad (11)$$

where,

$$\epsilon_{eff} = \epsilon_r - \frac{\epsilon_r - \epsilon_e}{1 + G \left(\frac{f_r}{f_p} \right)^2} \quad (12)$$

$$G = \left(\frac{Z_0 - 5}{60} \right)^{\frac{1}{2}} + (0.004 \times Z_0) \quad (13)$$

$$f_p = \frac{Z_0}{2\mu_0 h} \quad (14)$$

$$\mu_0 = 4\pi \times 10^{-9} \quad (15)$$

$$\text{and } \lambda_0 = \frac{c}{f_r} \text{ cm} \quad (16)$$

The 50Ω microstripline feed of length L_f and width W_f (designed as per the above procedure) will be connected at the center point (C_p) along the width W of the conventional rectangular radiating patch is shown in Fig (1). But the impedance offered by the patch at C_p may not be equal to 50Ω . Hence, microstripline feed need not be connected at this point as impedance

mismatch occurs. In such case a matching transformer must be used between C_p and 50Ω microstripline for better impedance matching.

5. Design of quarter wave transformer($\lambda_g/4$) :

A very important circuit element in most microstrip designs is the quarter wave transformer. As its length is one fourth of the guide wavelength (λ_g) so the name quarter wave transformer. The $\lambda_g/4$ transformer matches the impedance of two dissimilar sections. The impedance of $\lambda_g/4$ transformer

$$Z_t = \sqrt{Z_1 \times Z_3} \quad \Omega \quad (17)$$

Not only quarterwave transformer is used to match between two separate impedances, but also should be used wherever there is a possible impedance mismatch. Like for the single patch antenna, Z_t should be used between 50Ω microstripline feed and the input feed location C_p of the patch. For instant, the impedance at C_p along its width is 256.99Ω (obtained in the present study). This impedance is not same as that of the microstripline impedance of 50Ω . Therefore a quarter wave transformer may be used between the microstripline and center point C_p along the width of rectangular patch element for matching their impedances.

The following equations are used to determine the impedance R_{in} at C_p along the width of conventional RMA

$$R_{in} \cong \frac{(120\lambda_0)^2 + \left(\frac{377h}{\sqrt{\epsilon_r}L}\right)^2 \tan^2 \beta l}{240 \times L \times \lambda_0 (1 + \tan \beta l)} \quad \Omega \quad (18)$$

$$\text{where, } \beta = \frac{2\pi\sqrt{\epsilon_r}}{\lambda_0} \quad (19)$$

$$l = \frac{\theta\pi}{180\beta} = \frac{W}{2} \text{ cm} \quad (20)$$

Impedance of $\lambda_g/4$ transformer is given by $Z_t = \sqrt{R_{in} \times Z_0}$. The width of $\lambda_g/4$ transformer W_t is obtained by using equations (6) to (9). The length of $\lambda_g/4$ transformer L_t is obtained by using equations (10) to (16) by replacing Z_0 by Z_t .

The designed geometry of center fed single element RMSA is as shown in Fig. (1).

6. Design of ground plane:

The size of the ground plane is selected as per the following equations.

$$L_g = 6h + L \text{ cm} \quad (21)$$

$$W_g = 6h + W \text{ cm} \quad (22)$$

Fig (1) shows the geometry of reference antenna RMSA having length $L=11.33$ mm and the width $W = 15.22$ mm for 6 GHz operating frequency. The antenna uses a low cost glass epoxy substrate having relative permittivity of $\epsilon_r = 4.4$ and $\tan \delta = 0.0245$ and thickness $h = 1.6$ mm. The antenna is fed using microstripline feed through $\lambda_g/4$ transformer feed line of length $L_t=6.35$ mm and width $W_t=0.47$ mm. Microstripline is having feed length $L_s=6.29$ mm and width $W_s=3.16$ mm.

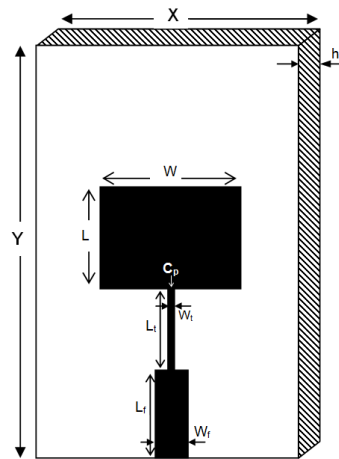
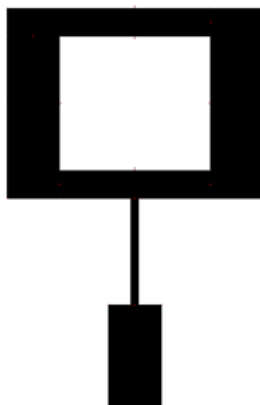
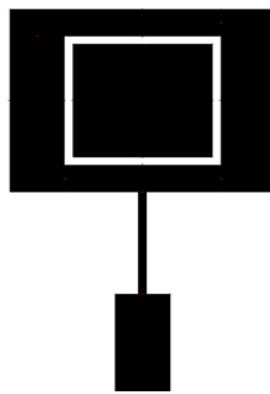


Fig. 1 Geometry of Reference Antenna; ANTo

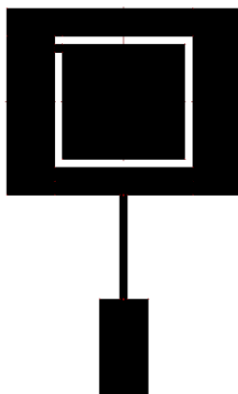
Fig (2) shows geometry of the proposed CCSR-SCS microstrip antenna, which is obtained by etching rectangular slot of dimension $L_1 = 8\text{mm} \times W_1 = 9\text{mm}$ and then placing a small patch $L_2 = 7\text{mm} \times W_2 = 8\text{mm}$ at the centre of the RMA and the ring so obtained is split by placing 0.5mm copper material at the corner, further a split C slot is embedded in the existing design by leaving 0.25mm from perimeter, along the length and 0.5mm along the width of the patch and etching 0.5mm copper material from the patch.



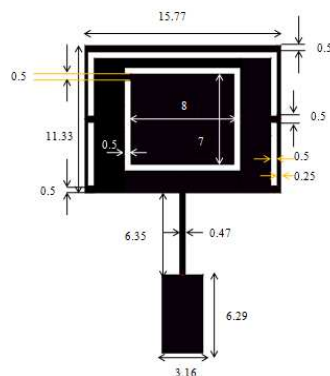
(a)ANT1



(b)ANT2



(c)ANT3



(d)ANT4



(e) Fabricated antenna

Fig. 2 Schematic representation and step by step evolution of the Proposed CCSR-SCS Antenna(ANT1 to ANT4);

(a)ANT1 (b)ANT2 (c)ANT3 (d)ANT4(e) Fabricated antenna

III Results and discussions

Mentor graphics 3DEM software is used to simulate the proposed CCSR-SCS antenna and later the simulated results are validated using Vector Network Analyser. Table 1 shows the comparison of simulated and validated results of reference Rectangular microstrip antenna (RMSA) antenna and proposed CCSR-SCS antenna.

Table 1 Performance of the proposed antenna.

| Antenna Configuration | Resonant Frequency(GHz) | | Return Loss (dB) | | Bandwidth (MHz) | | Size Reduction in % |
|-----------------------|-------------------------|----------|------------------|----------|-----------------|----------|---------------------|
| | Simulated | Measured | Simulated | Measured | simulated | Measured | |
| RMSA | 5.92 | 5.87 | -14.76 | -13.00 | 155 | 150 | NA |
| | 2.47 | 2.60 | -17.4 | -12.18 | 45 | 200 | 60 |
| | 3.44 | 3.40 | -20.2 | -32.58 | 49 | 140 | 44 |
| CCSR-SCS | 3.99 | 4.00 | -10.7 | -13.03 | 30 | 60 | 35 |
| | 5.5 | 5.40 | -34.1 | -26.73 | 137 | 130 | 9 |
| | 8.1 | 8.47 | -23.1 | -20.21 | 260 | 310 | NA |
| | 10.1 | 10.3 | -21.5 | -11.85 | 223 | 70 | NA |

It is evident from the table that the resonant frequency of CCSR-SCS has decreased significantly thereby giving a size reduction of 60% and Hexaband resonance. It is further seen from the table that simulated and measured results are in good agreement. The same can be confirmed from Fig(3).

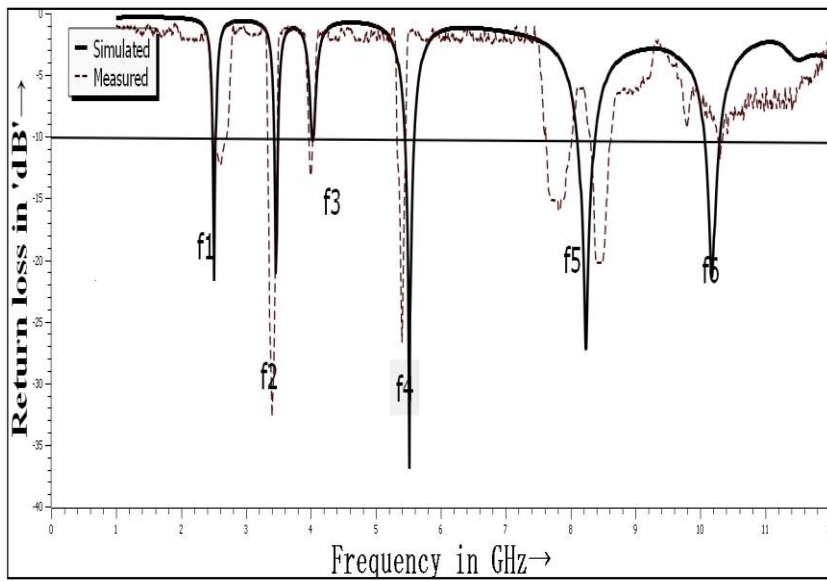
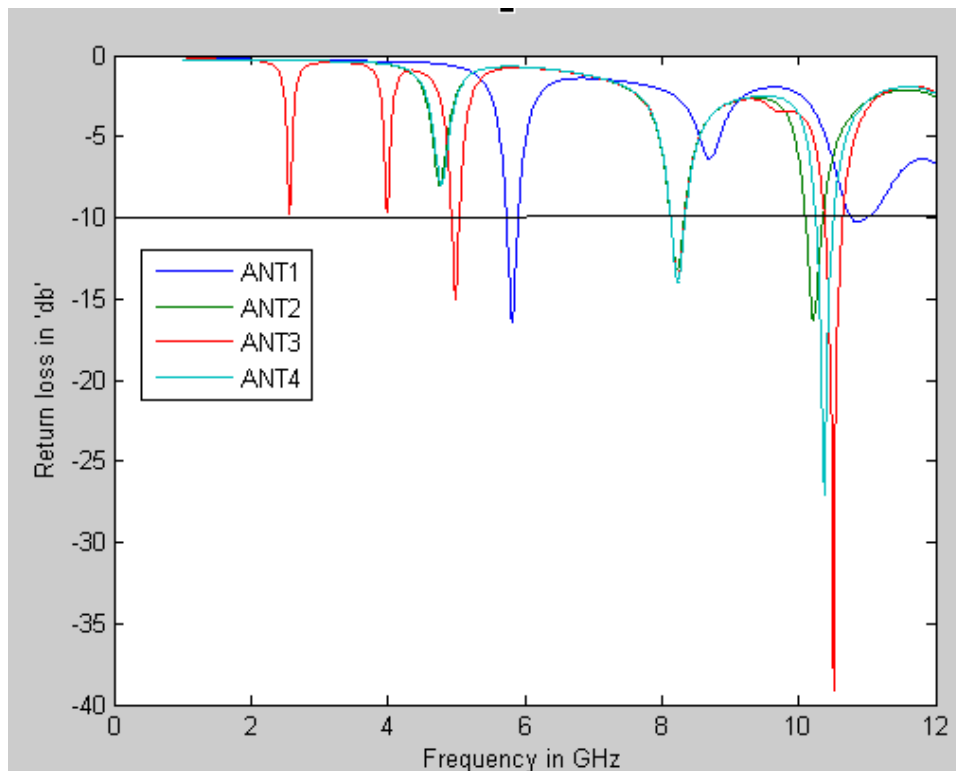


Fig. 3 Simulation and Experimental return loss of the proposed CCSR-SCS antenna



Fig(4)Simulation results of ANT1,ANT2,ANT3,ANT4

Fig(4) Shows the returnloss characteristic of ANTO(reference antenna) resonating at 6GHz. Ant1 resonates at 8.2GHz and 10.2GHz leading to dual bands,Ant2 resonates at 8.1 GHz ,10.4 GHz and there is a possibility of resonance at 4.7GHz.Ant3 resonates at 5 GHz ,8.2 GHz and 10.5 GHz with a possibility of resonance at 2.5 GHz and 4 GHz.

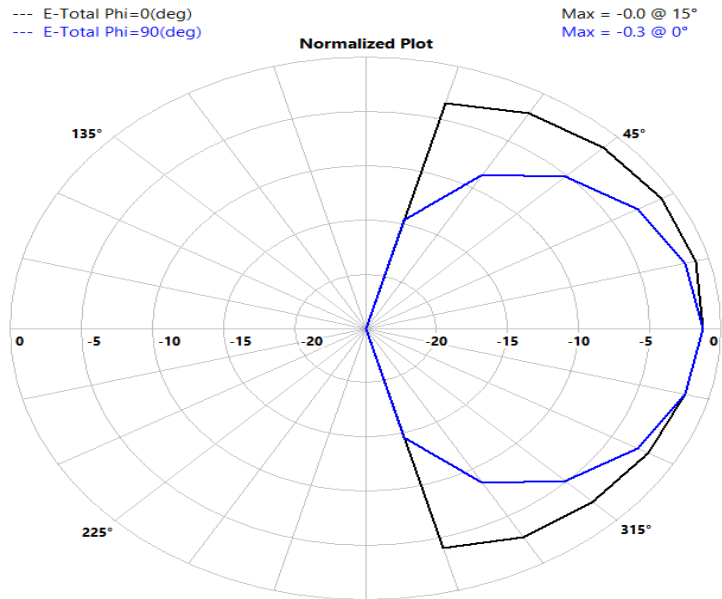


Fig (5). Radiation pattern of reference Antenna at 6GHz

The radiation pattern of reference antenna is shown in Fig(5). Further radiation pattern of proposed antenna at different frequencies of 2.47 GHz, 3.44 GHz, 3.99 GHz, 5.5 GHz, 8.1 GHz and 10.1 GHz are shown in Fig (6), Fig(7), Fig(8), Fig(9), Fig(10) and Fig(11) respectively. The radiation behavior of the antenna in the two principle planes, including the lower and higher end of the impedance bandwidth shows the patterns are stable and resemble like broadside antenna radiation pattern in the entire operational band and highly suitable for the wireless communication system applications.

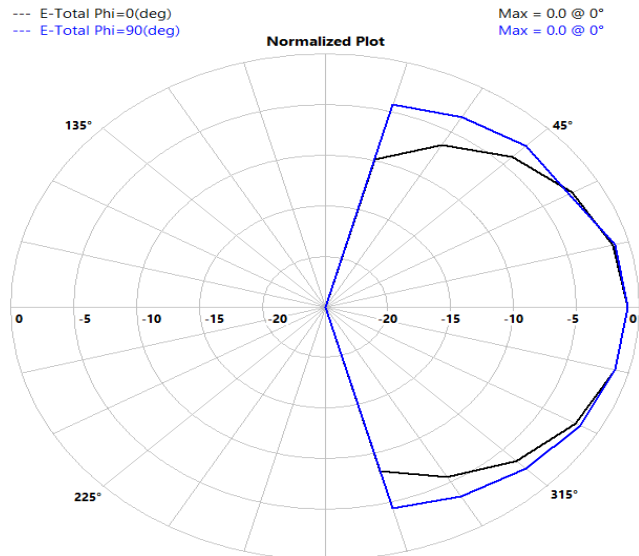


Fig (6). Radiation pattern of CCSR-SCS Antenna at 2.47GHz

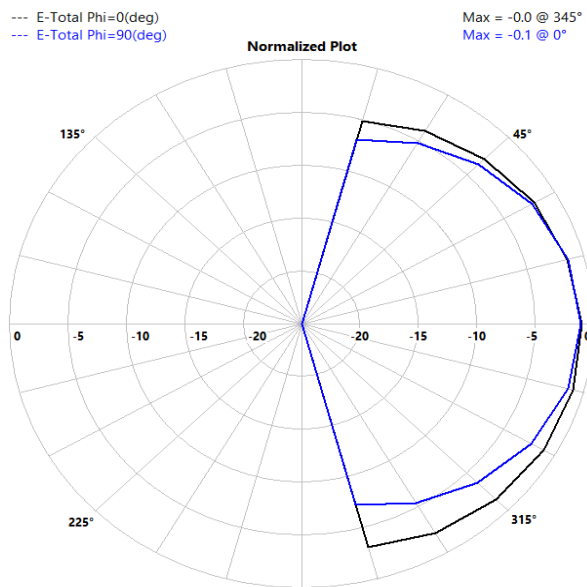


Fig (7). Radiation pattern of CCSR-SCS Antenna at 3.44GHz

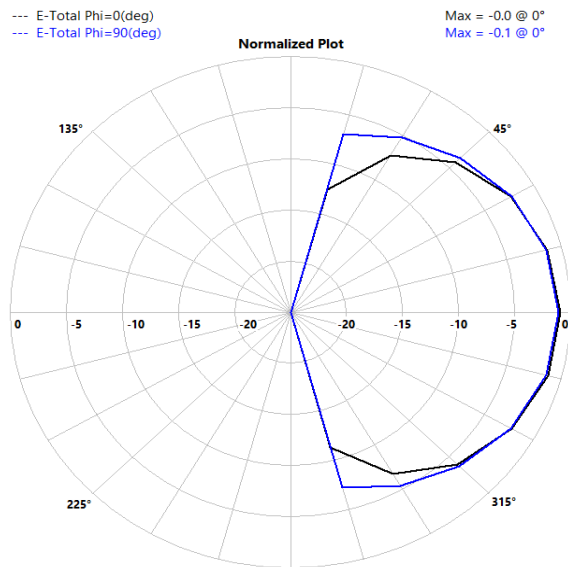


Fig (9). Radiation pattern of CCSR-SCS Antenna at 5.5GHz

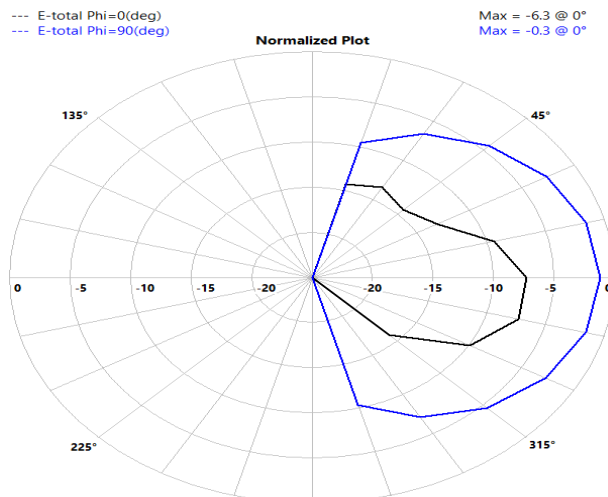


Fig (10). Radiation pattern of CCSR-SCS Antenna at 8.1GHz

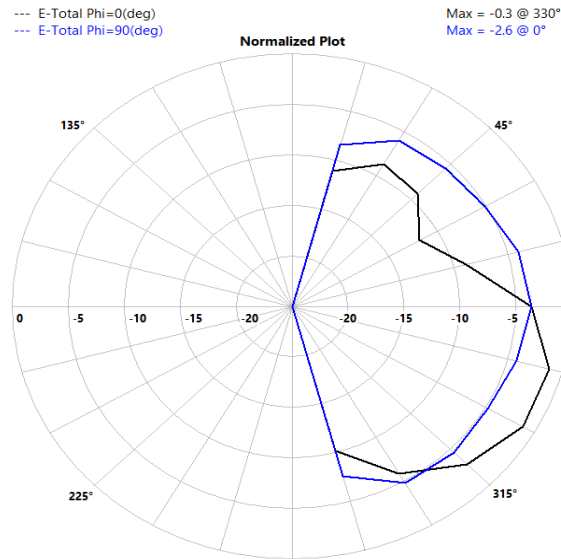


Fig (11). Radiation pattern of CCSR-SCS Antenna at 10.1GHz

Further Current distribution of proposed antenna at different frequencies of 2.47 GHz, 3.44 GHz, 3.99 GHz, 5.5 GHz, 8.1 GHz and 10.1 GHz are shown in Fig (12), Fig(13), Fig(14), Fig(15), Fig(16) and Fig(17) respectively. Current is much stronger around the edges of the CCSR-SCS antenna along with uniform distribution of current over entire patch indicating that patch size plays important role at lower frequencies and current distribution for upper bands is mainly from the split ring as strong current distribution moves towards the center of the patch.

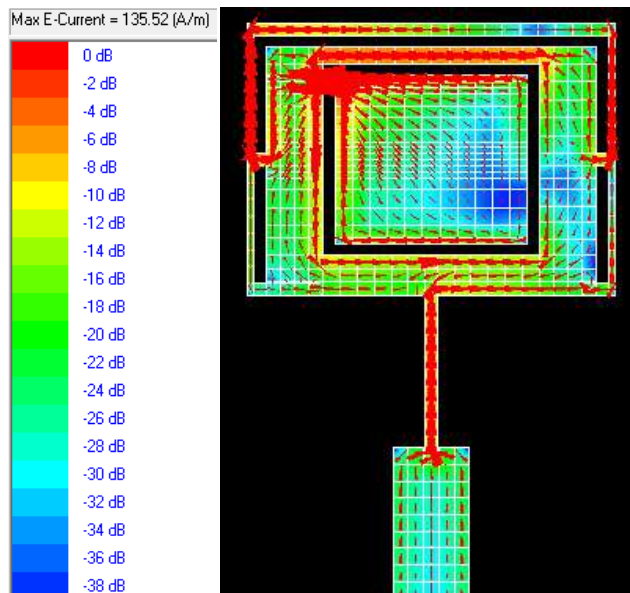


Fig (12). Current distribution of CCSR-SCS Antenna at 2.47GHz

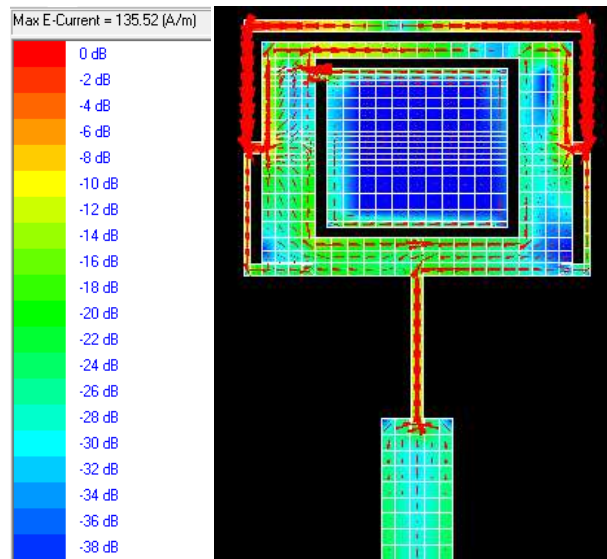


Fig (13). Current distribution of CCSR-SCS Antenna at 3.44GHz

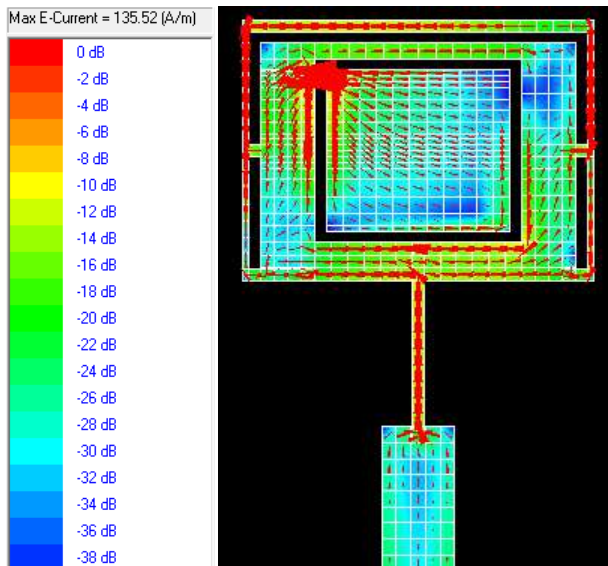


Fig (14). Current distribution of CCSR-SCS Antenna at 3.99 GHz

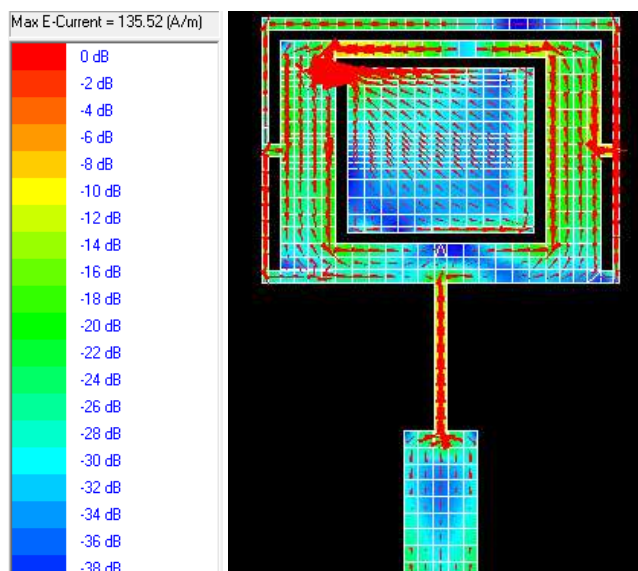


Fig (15). Current distribution of CCSR-SCS Antenna at 5.5 GHz

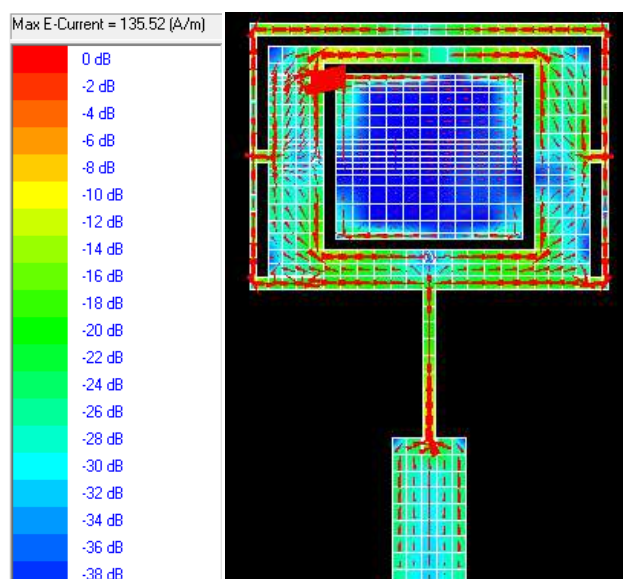


Fig (16). Current distribution of CCSR-SCS Antenna at 8.1 GHz

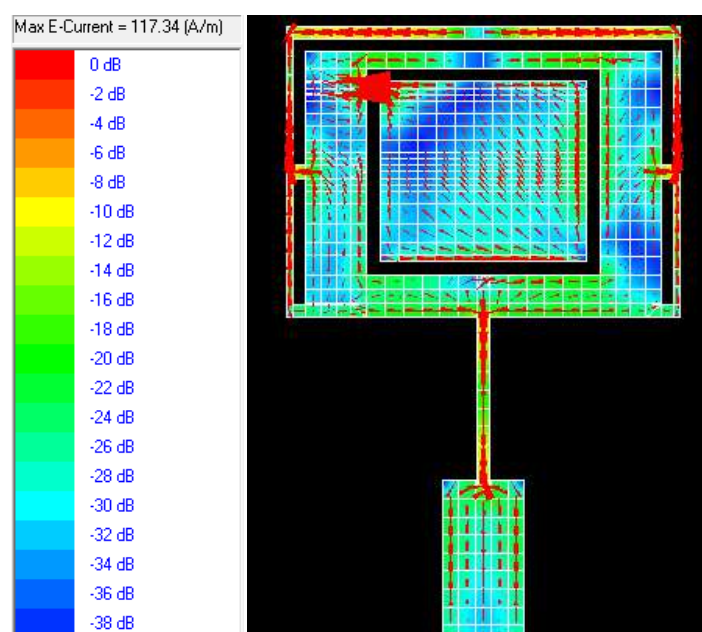


Fig (17). Current distribution of CCSR-SCS Antenna at 10.1 GHz

IV. CONCLUSIONS

A CCSR-SCS antenna is studied. Simulation and Validation results are in good agreement. It has been observed that CCSR-SCS gives a size reduction of 60% along with Hexabands, the compactness is due to larger path length of surface current. The radiation patterns of all proposed antennas are of broadside in nature.

V. ACKNOWLEDGMENT

I would like to thank Chancellor, Vice-chancellor and all the office bearers of Sharnbasva University and Chairman of E&CE department for extending the support.

REFERENCES

- [1] S. Baligar, U. K. Revankar and K. V. Acharya. (Oct 2000). Broadband stacked annular ring Coupled shorted Circular microstrip antenna. *Electronic Letters* 36(21),1756-1757. <http://dx.doi.org/10.1049/el:20001286>
- [2] J. S. Baligar, U. K. Revankar and K. V. Acharya. (2001). Broadband two layer Shorted patch Antenna with low cross polarization. *Electronic Letters*, 3(9), 547-548. <http://dx.doi.org/10.1049/el:20010371>
- [3] Amit A. Deshmukh and Girish Kumar. (2001). Compact broadband Gap-coupled Square ring and W-shaped Microstrip antennas. *International RADAR Symposium*. (pp 853-86). <https://doi.org/10.1002/mop.21671>
- [4] R. Garg, P. Bhartia, I. Bahl, A. Ittipiboon. (2001). *Microstrip Antenna Design Handbook*. Artech House.
- [5] T. S. P. sec, Zhi Ning chen. (Aug 2002). Slot- loaded center-Fed Microstrip patch antenna. *Microwave and optical Technology Letters*. Vol. 34, No.3, pp 227-23. <https://doi.org/10.1002/mop.10424>
- [6] C. A. Balanis. (2005). *Antenna Theory_Analysis and Design*. John Wiley & Sons.
- [7] Revansiddappa S. K., Ravi M. Yadahalli and Siddarama R Patil. (2016). Compact ring coupled Multi band Rectangular Microstrip patch antenna with C-Slot. *Antenna Test & Measurement Society (ATMS India-16)*.(pp: 1-3).
- [8] Nasimuddin N, Chen ZN and Xianming Q (2010) Dual-band circularly polarized S-shaped slotted patch antenna with a small frequency-ratio. *IEEE Transactions on Antennas and Propagation* 58, 2112–2115.doi:10.1109/tap.2010.2046851.
- [9] Chaurasia P, Kanaujia BK, Dwari S, Khandelwal MK (2018). Penta- band microstrip patch antenna with small frequency ratios using metamaterial for wireless applications. *International Journal of Microwave and Wireless Technologies* 1–10. <https://doi.org/10.1017/S1759078718000570>.
- [10] Chen, H., Yang, X., Yin, Y. Z., Fan, S. T., & Wu, J. J. (2013). Triband planar monopole antenna with compact radiator for WLAN/WiMAX applications. *IEEE Antennas and Wireless Propagation Letters*, 12, 1440–1443. doi:10.1109/lawp.2013.2287312
- [11] Amit A. Deshmukh & Priyanka Verma (2019): Multi-band Dual Polarized Variations of Modified Circular Microstrip Antennas, *IETE Journal of Research*, DOI:10.1080/03772063.2019.1604179
- [12] Y. L. Kuo, and K. L. Wong,(2003) “Printed double-T monopole antenna for2.4/5.2 GHz dual-band WLAN operations,” *IEEE Trans. Anten- nasPropag.*, Vol. 51, pp. 2187_91,
- [13] W. C. Liu,(2007) “Optimal design of dual band CPW-FED G-shaped monopole antenna for WLAN application,” *Prog. Electromagn. Res.*,Vol. 74, pp. 21_38.
- [14] Z. Y. Liu, Y. Z. Yin, L. H. Wen, W. C. Xiao, Y. Wang, and S. L. Zuo,(2010) “A Yshaped tri-band monopole antenna with a parasitic M-strip for PCS and WLAN applications,” *J. Electromagn. Waves Appl.*, Vol. 24, pp. 1219_27.

- [15] Anantha Bharathi, Lakshminarayana Merugu & P. V. D. Somasekhar Rao (2020) Reconfigurable Corner Truncated Square Microstrip Patch Antennas for Wireless Communication Applications, *IETE Journal of Research*, 66:2, 242-255, DOI:10.1080/03772063.2018.1478326.
- [16] Mak, A.C.K.; Rowell, C.R.; Murch, R.D.; Mak, C.L (2007),.: Reconfigurable multiband antenna designs for wireless communication devices. *IEEE Trans. Antennas Propag.*, Vol. 55 1919–1928.
- [17] Shirazi, M.; Li, T.; Gong, X(2015).: Effects of PIN Diode Switches on The Performance of Reconfigurable Slot-Ring Antenna. *IEEE Wireless and Microwave Technology Conf.(WAMICON)*, Florida, USA,
- [18] Paul, P. M., Kandasamy, K., & Sharawi, M. S. (2018). A Tri-band Circularly Polarized Strip and SRR Loaded Slot Antenna. *IEEE Transactions on Antennas and Propagation*. <https://idr.nitk.ac.in/jspui/handle/123456789/9760>
- [19] Rajkumar R., & Usha Kiran, K. (2017). A Metamaterial Inspired Compact Open Split Ring Resonator Antenna for Multiband Operation. *Wireless Personal Communications*, 97(1), 951–965. doi:10.1007/s11277-017-4545-0
- [20] Rajesh Kumar, Malay Ranjan Tripathy & Daniel Ronnow (2018): Multi-resonant Bowtie Antenna with Modified Symmetric SRR for Wireless Applications, *IETE Journal of Research*, DOI: 10.1080/03772063.2018.1479663
- [21] Puente, C., Romeu, J., Pous, R., Garcia, X., & Benitez, F. (1996). Fractal multiband antenna based on the Sierpinski gasket. *Electronics Letters*, 32(1), 1. doi:10.1049/el:19960033
- [22] J. Malik, P. C. Kalaria, and M. V. Kartikeyan, (2013) “Complementary Sierpinskigasket fractal antenna for dual-band WiMAX/WLAN (3.5/5.8 GHz) applications,” *Int. J. Microw. Wirel. Technol.*, Vol. 5, pp. 499_505.
- [23] Singh, D. K., Kanaujia, B. K., Dwari, S., Pandey, G. P., & Kumar, S. (2015). Multiband Circularly Polarized Stacked Microstrip Antenna. *Progress In Electromagnetics Research C*, 56, 55–64. doi:10.2528/pierc14121101.
- [24] Vani, R. M., Naveen, S. M., & Hunagund, P. V. (2012). Stacked compact ring-coupled rectangular microstrip antenna for multiband applications. *Microwave and Optical Technology Letters*, 54(6), 1387–1391. doi:10.1002/mop.26842.



Revansiddappa S. Kinagi received Bachelor of Engineering in Electronics and Communication Engineering from Visvesvaraya Technological University(VTU) Belagavi ,Karnataka ,India.in 2004 and received Master of Technology in Digital Electronics from VTU in 2007.He is working as Associate Professor at Sharnbasva University Kalaburagi,Karnataka,India.His main research interests are Microstrip patch antennas,Wireless communication and Microwave Engineering.



Ravi M. Yadahalli received Bachelor of Engineering in Electronics and Communication Engineering from Gulbarga University, Kalaburagi, Karnataka, India in 1990, and received Master of Technology in Power Electronics from Gulbarga University, Kalaburagi, Karnataka, India in 1993 and Ph.D. from Gulbarga University, Kalaburagi, Karnataka, India in 2009. He is working as Professor at Hirasugar Institute of Technology, Nidasoshi, Belagavi, India. His main research interests are Microstrip patch antennas, Wireless sensor Networks and Microwave Engineering.



Siddarama R. Patil received Bachelor of Engineering in Electronics and Communication Engineering from Gulbarga University, Gulbarga, Karnataka, India in 1990, received Master of Technology in Telecommunication System Engineering from IIT Kharagpur in 1999 and Ph.D. from IIT Kharagpur in 2009. He is working as Professor, Dean of Academics in E&CE department PDA College of Engineering, Kalaburagi, Karnataka, India. His main research interests are Information Theory and Coding, Turbo Codes, LDPC codes, Iterative decoding algorithms, wireless communication wireless sensor network, Ad-Hoc Networks.

Figures

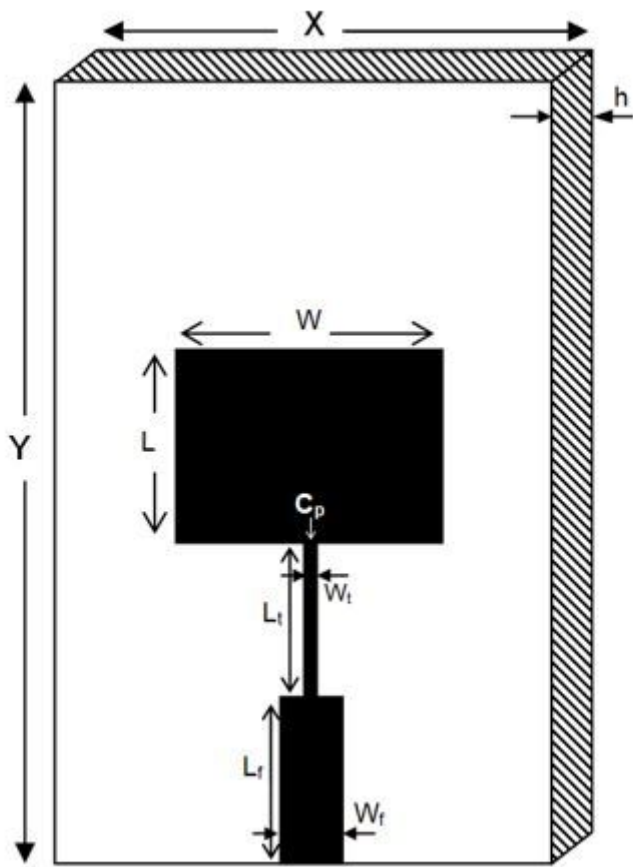
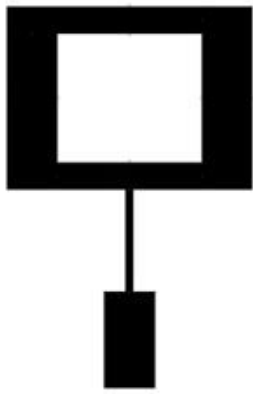
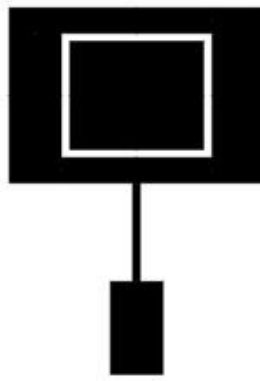


Figure 1

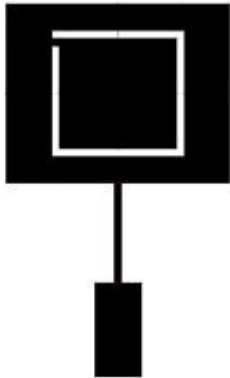
Geometry of Reference Antenna;ANT0



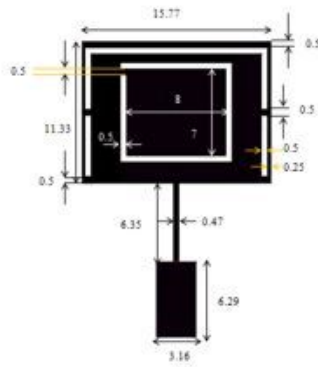
(a)ANT1



(b)ANT2



(c)ANT3



(d)ANT4



(e) Fabricated antenna

Figure 2

Schematic representation and step by step evolution of the Proposed CCSR-SCS Antenna(ANT1 to ANT4); (a)ANT1 (b)ANT2 (c)ANT3 (d)ANT4(e) Fabricated antenna

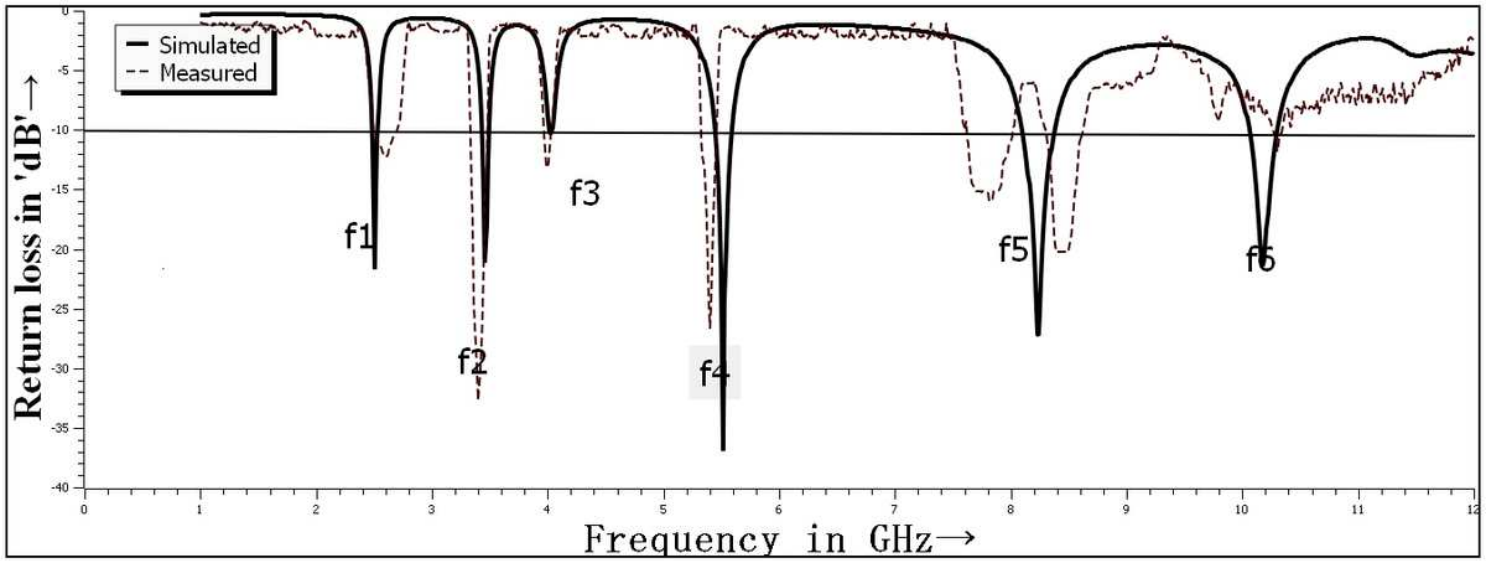


Figure 3

Simulation and Experimental return loss of the proposed CCSR-SCS antenna

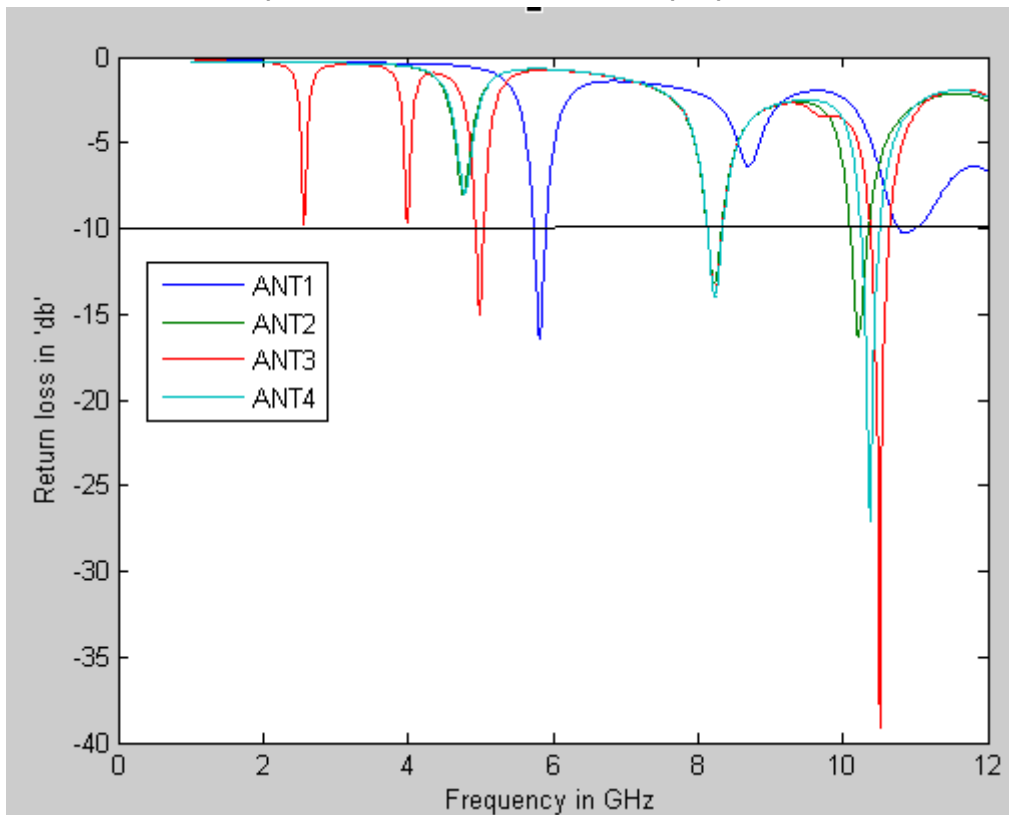


Figure 4

Simulation results of ANT1,ANT2,ANT3,ANT4

--- E-Total Phi=0(deg)
--- E-Total Phi=90(deg)

Max = -0.0 @ 15°
Max = -0.3 @ 0°

Normalized Plot

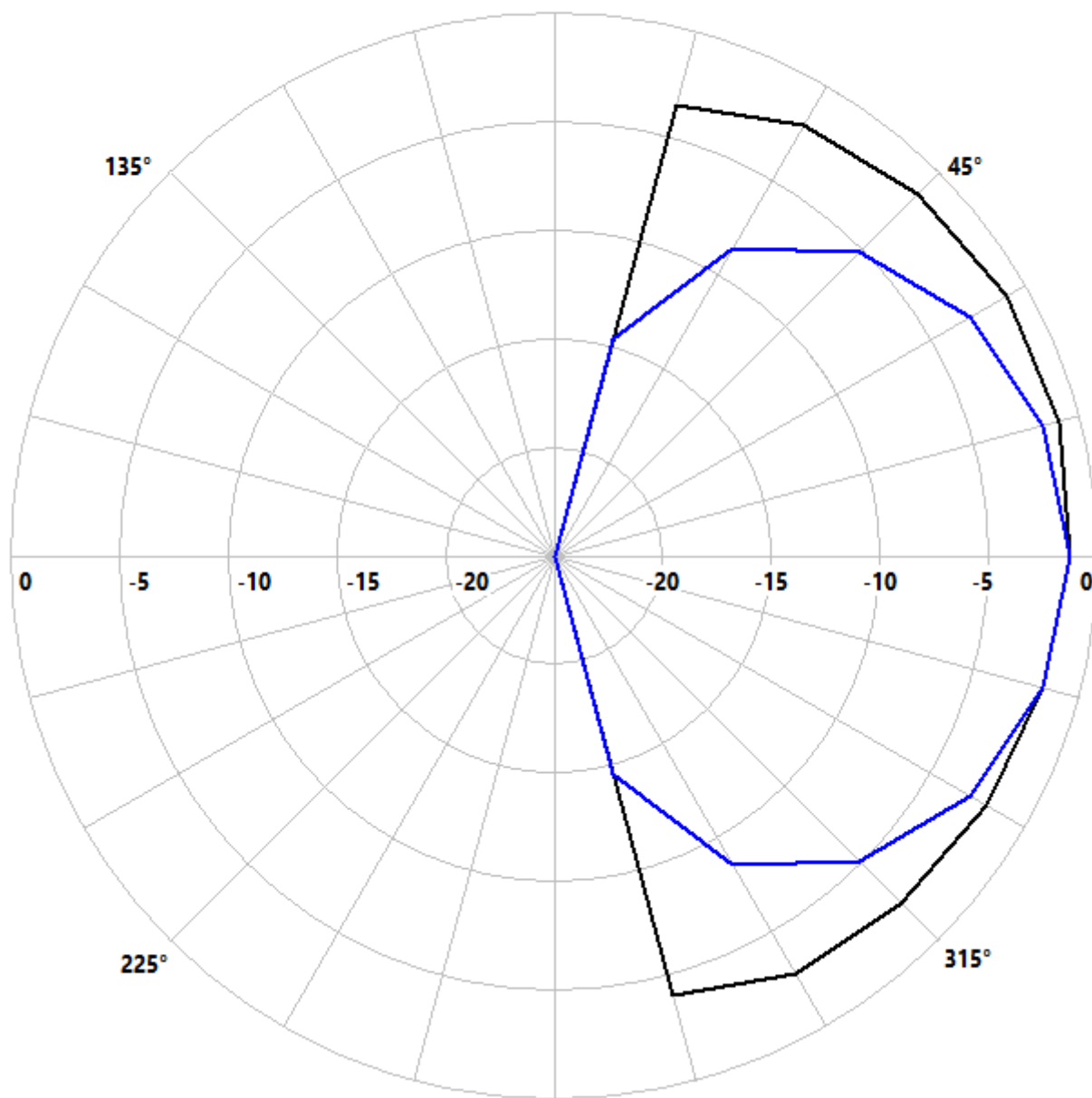


Figure 5

Radiation pattern of reference Antenna at 6GHz

--- E-Total Phi=0(deg)
--- E-Total Phi=90(deg)

Max = 0.0 @ 0°
Max = 0.0 @ 0°

Normalized Plot

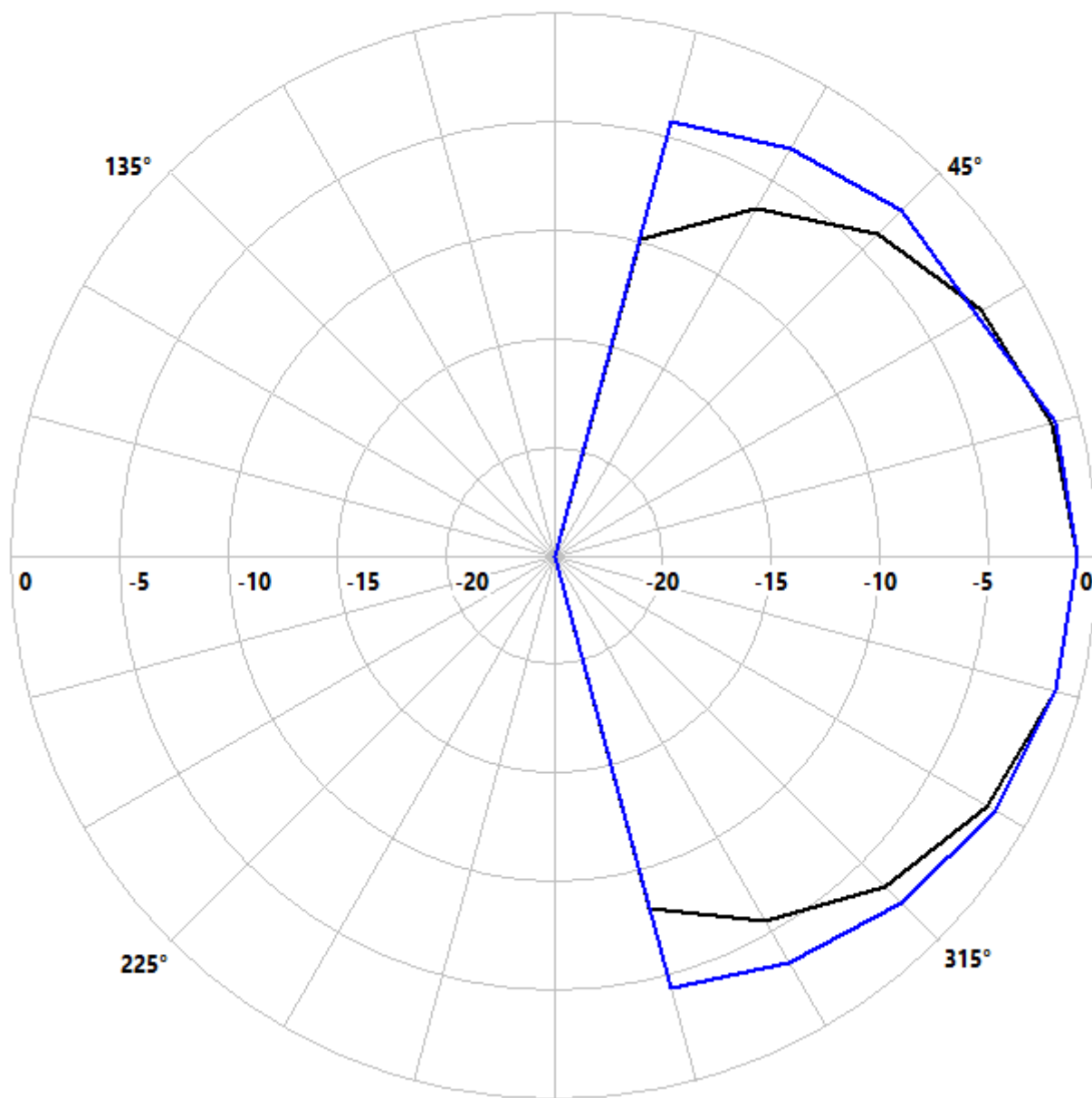


Figure 6

Radiation pattern of CCSR-SCS Antenna at 2.47GHz

--- E-Total Phi=0(deg)
--- E-Total Phi=90(deg)

Max = -0.0 @ 345°
Max = -0.1 @ 0°

Normalized Plot

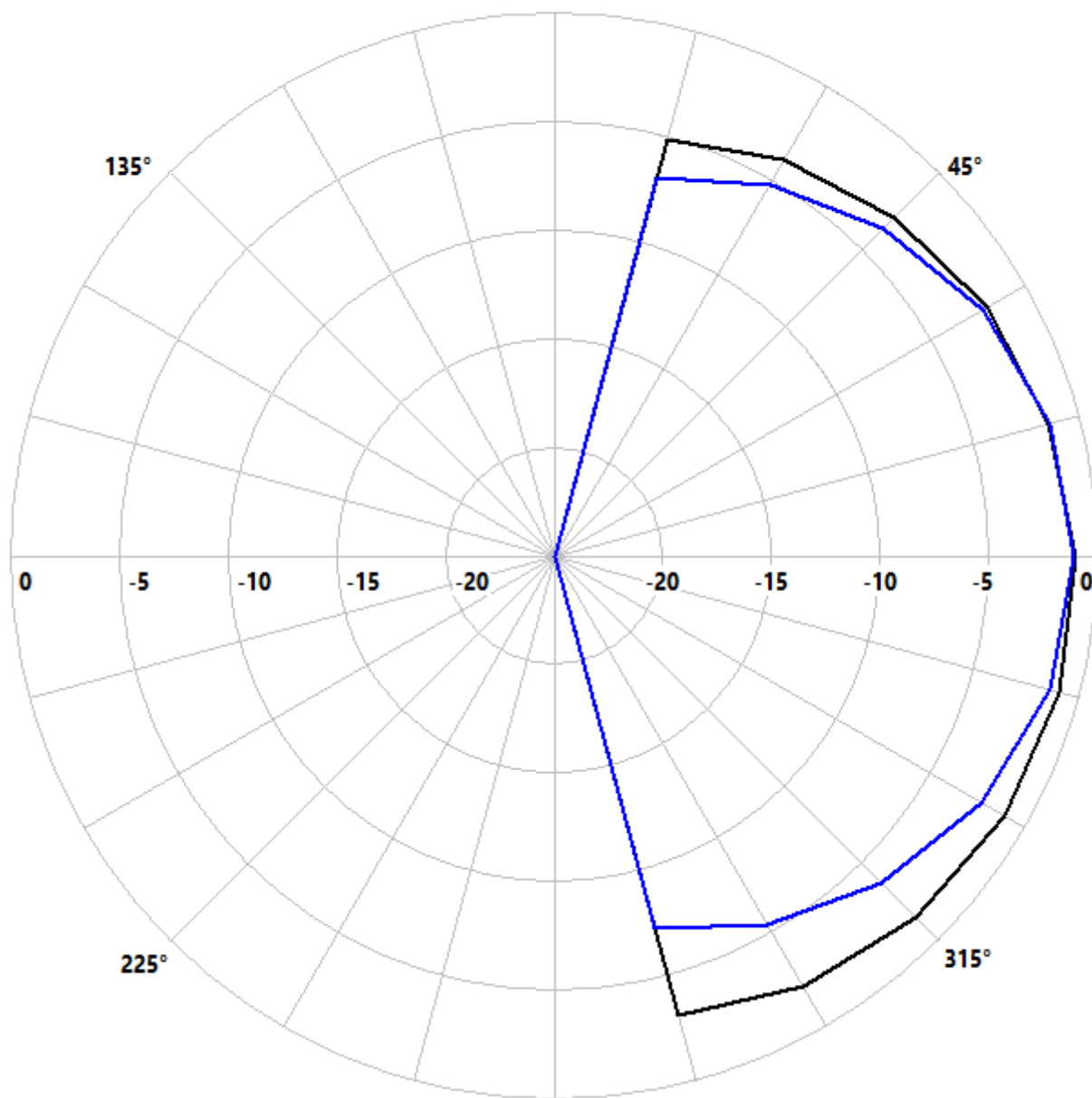


Figure 7

Radiation pattern of CCSR-SCS Antenna at 3.44GHz

Image not available with this version

Figure 8

Figure 8

--- E-Total Phi=0(deg)
--- E-Total Phi=90(deg)

Max = -0.0 @ 0°
Max = -0.1 @ 0°

Normalized Plot

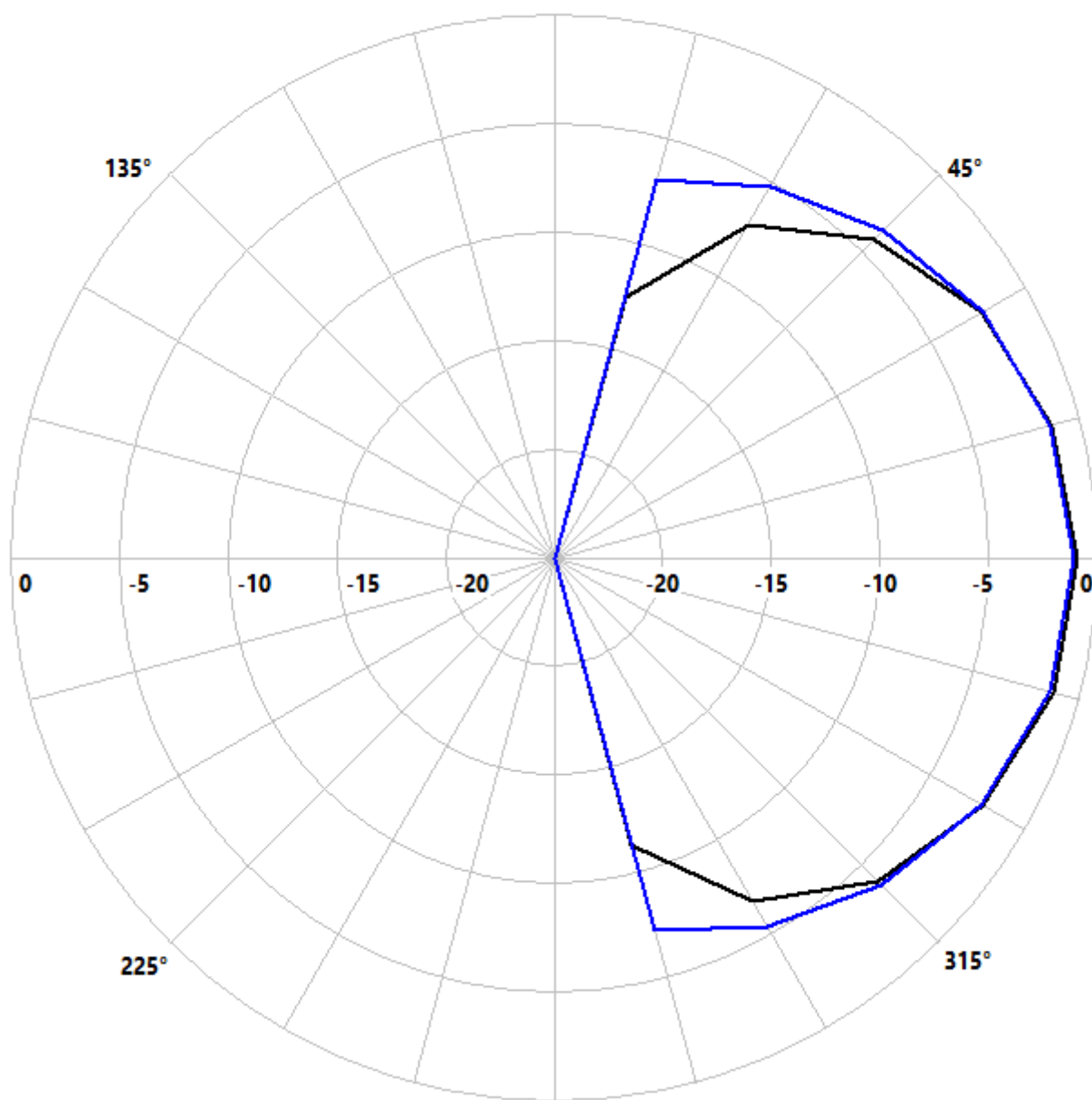


Figure 9

Radiation pattern of CCSR-SCS Antenna at 5.5GHz

--- E-total Phi=0(deg)
--- E-total Phi=90(deg)

Max = -6.3 @ 0°
Max = -0.3 @ 0°

Normalized Plot

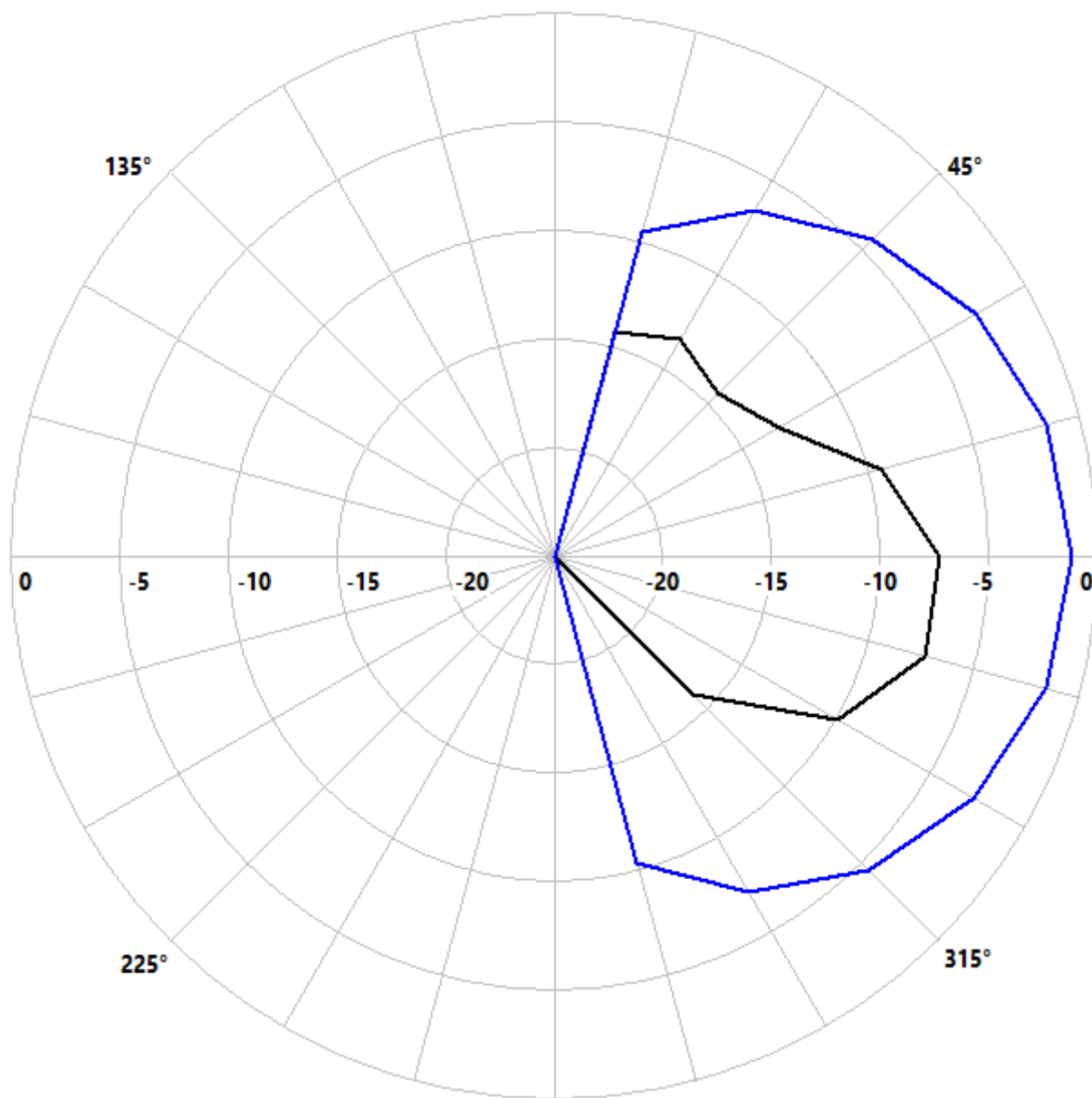


Figure 10

Radiation pattern of CCSR-SCS Antenna at 8.1GHz

--- E-Total Phi=0(deg)
--- E-Total Phi=90(deg)

Max = -0.3 @ 330°
Max = -2.6 @ 0°

Normalized Plot

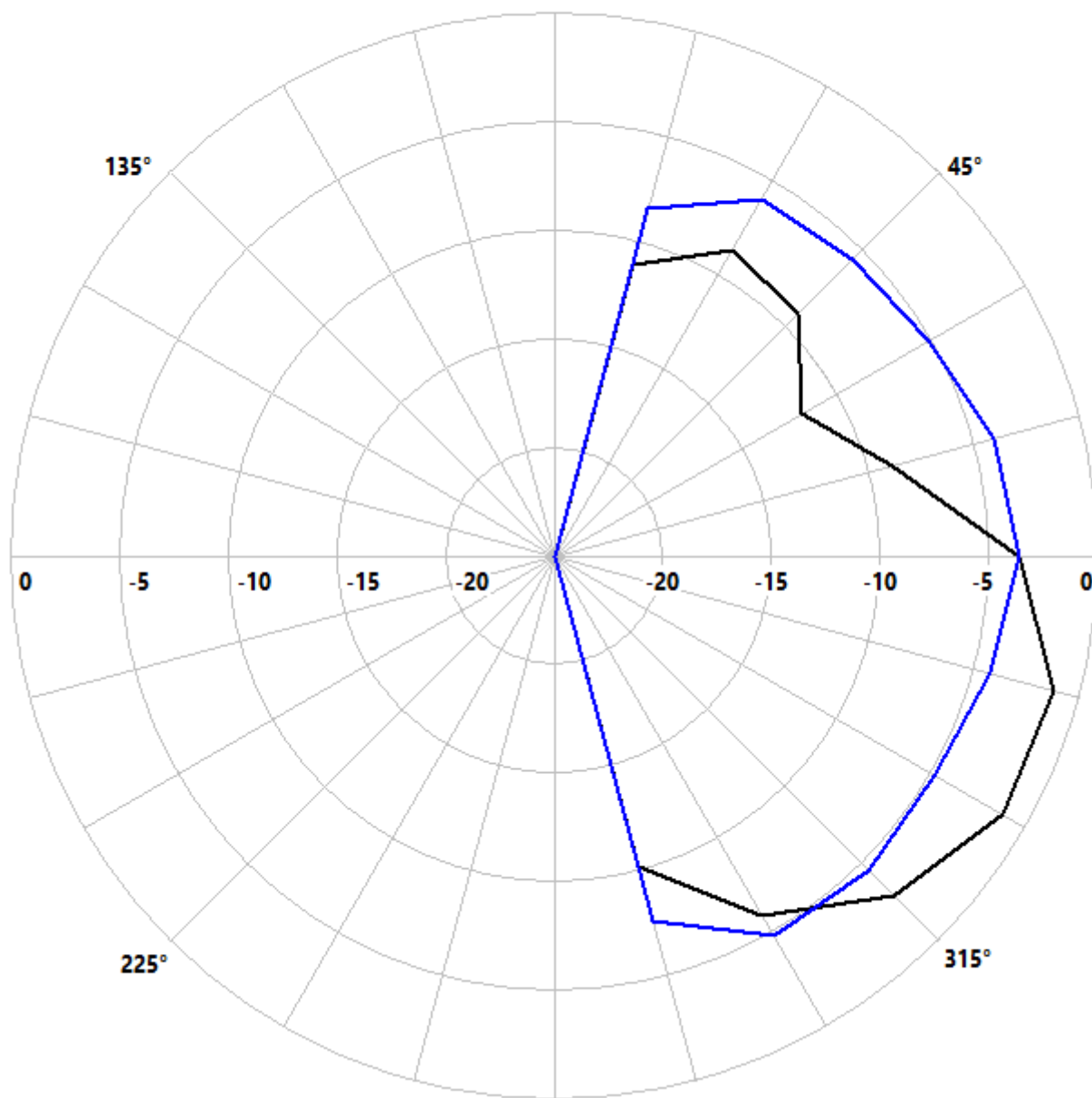


Figure 11

Radiation pattern of CCSR-SCS Antenna at 10.1GHz

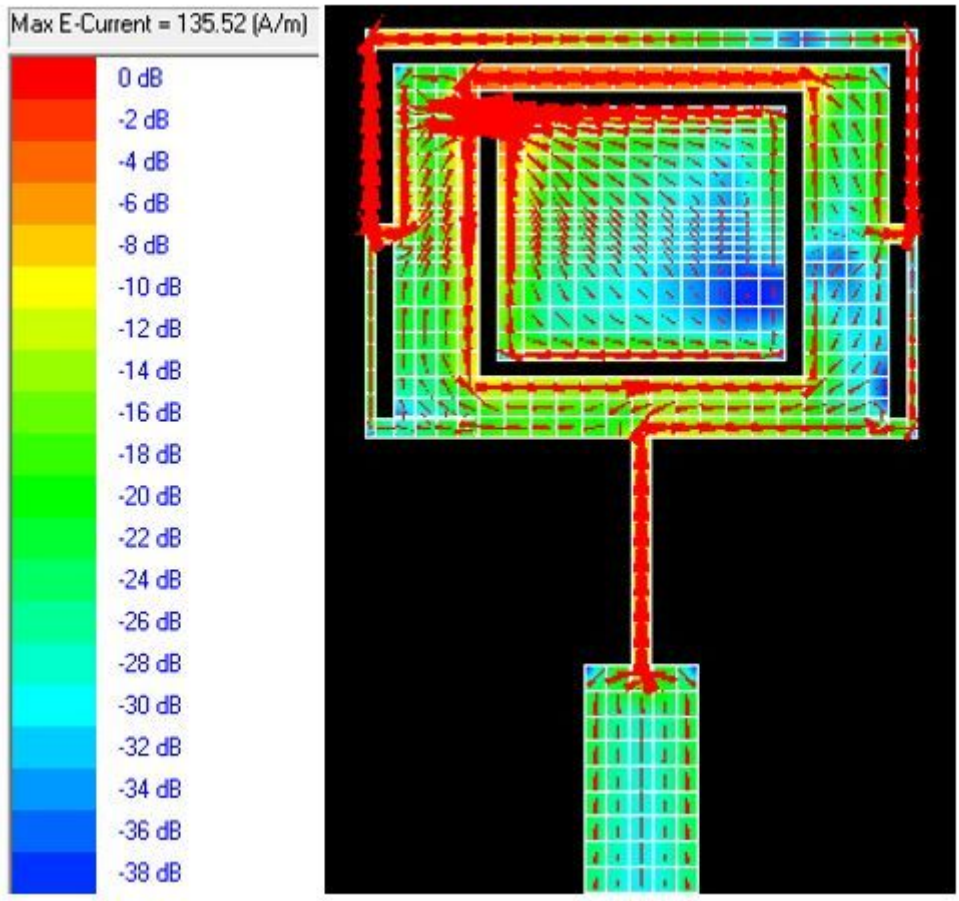


Figure 12

Current distribution of CCSR-SCS Antenna at 2.47GHz

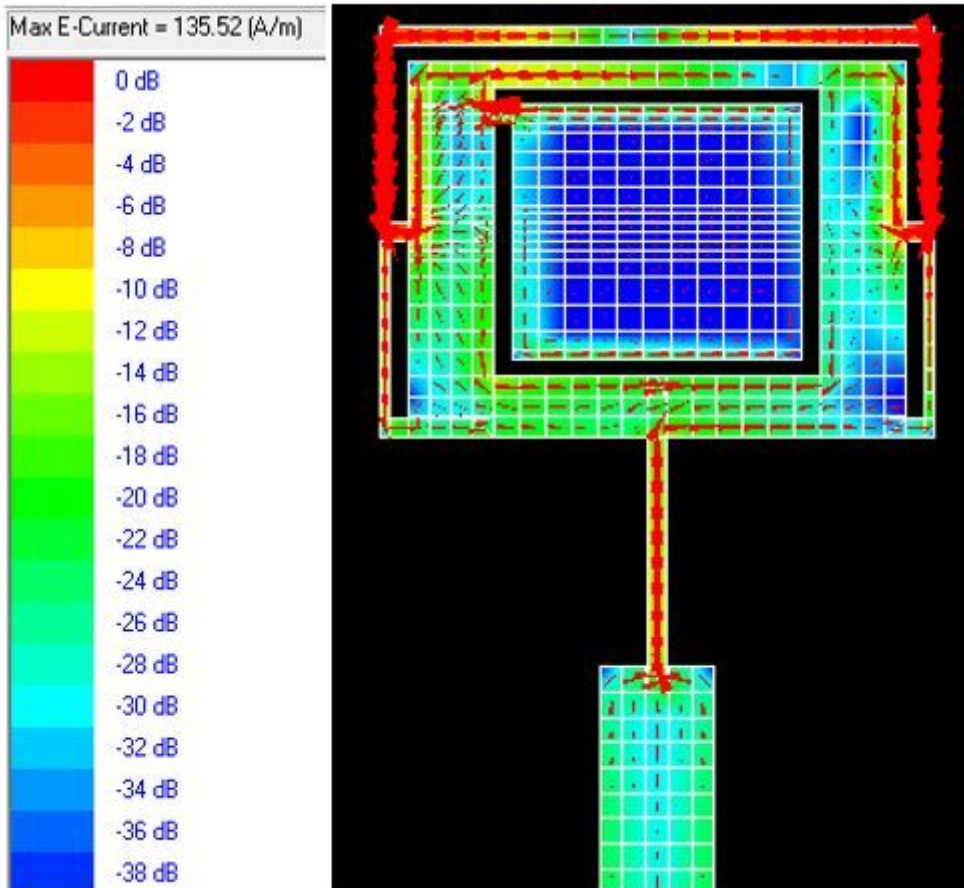


Figure 13

Current distribution of CCSR-SCS Antenna at 3.44GHz

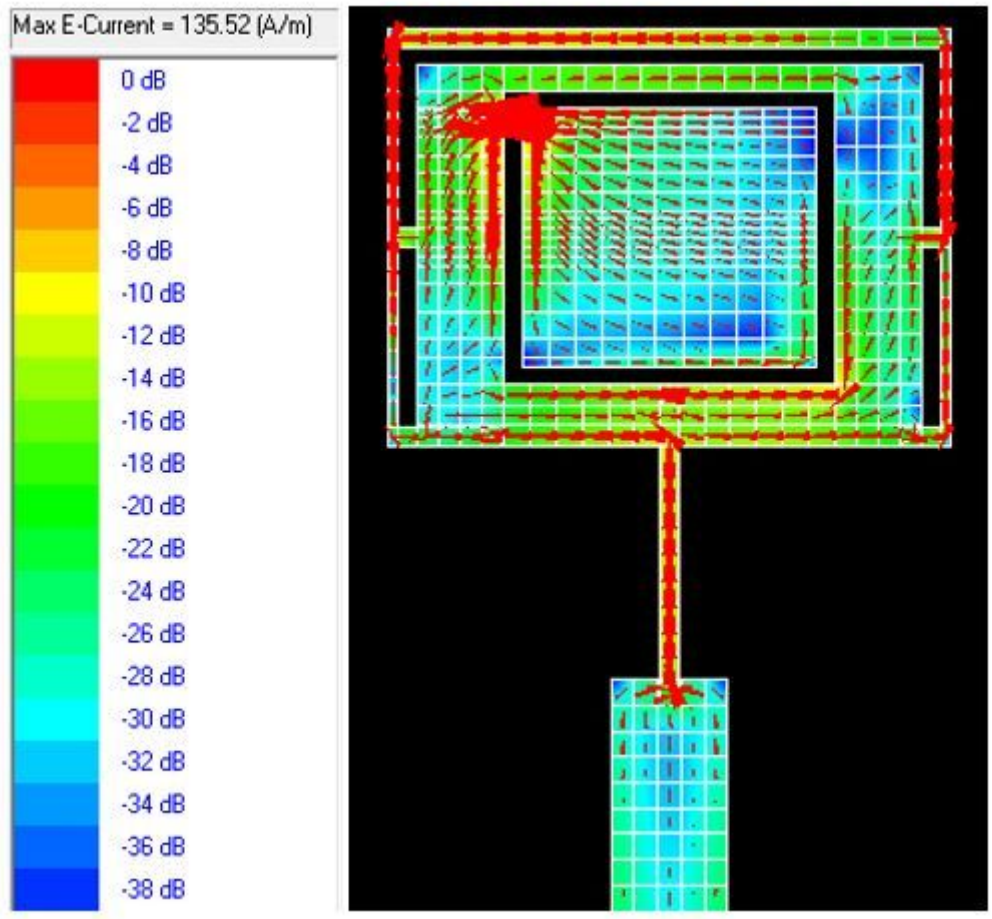


Figure 14

Current distribution of CCSR-SCS Antenna at 3.99 GHz

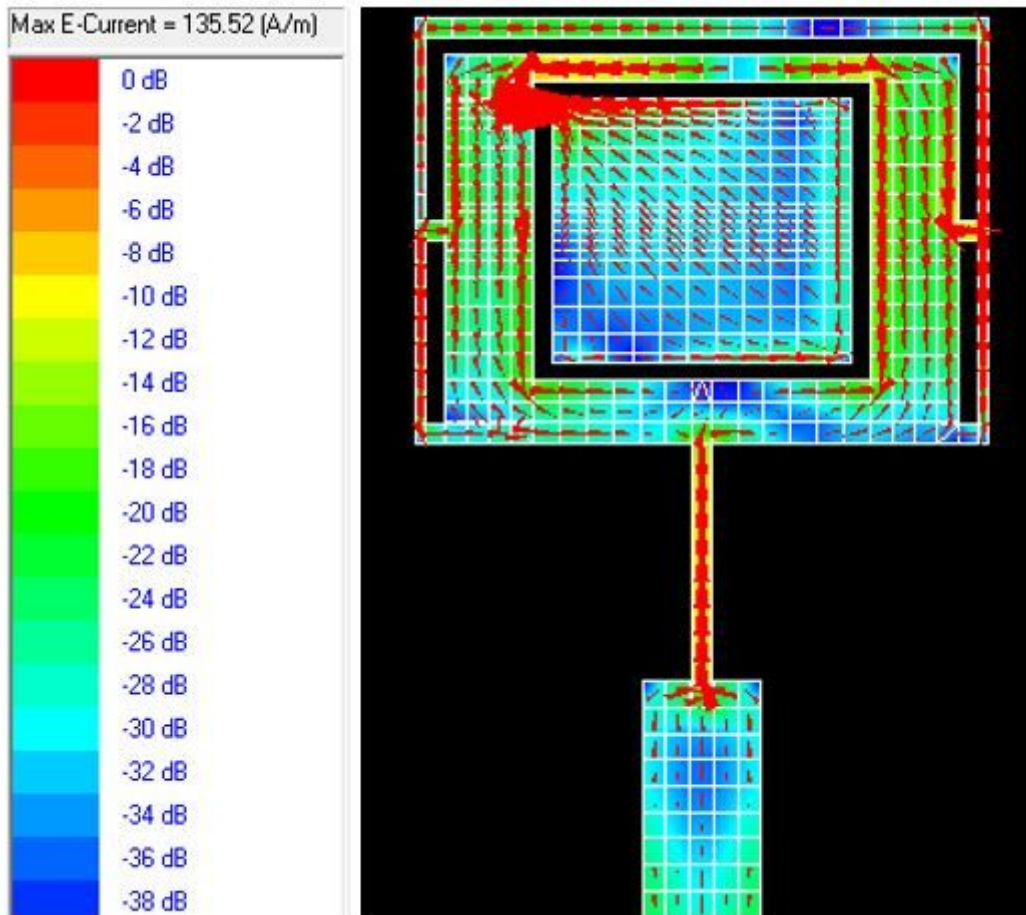


Figure 15

Current distribution of CCSR-SCS Antenna at 5.5 GHz

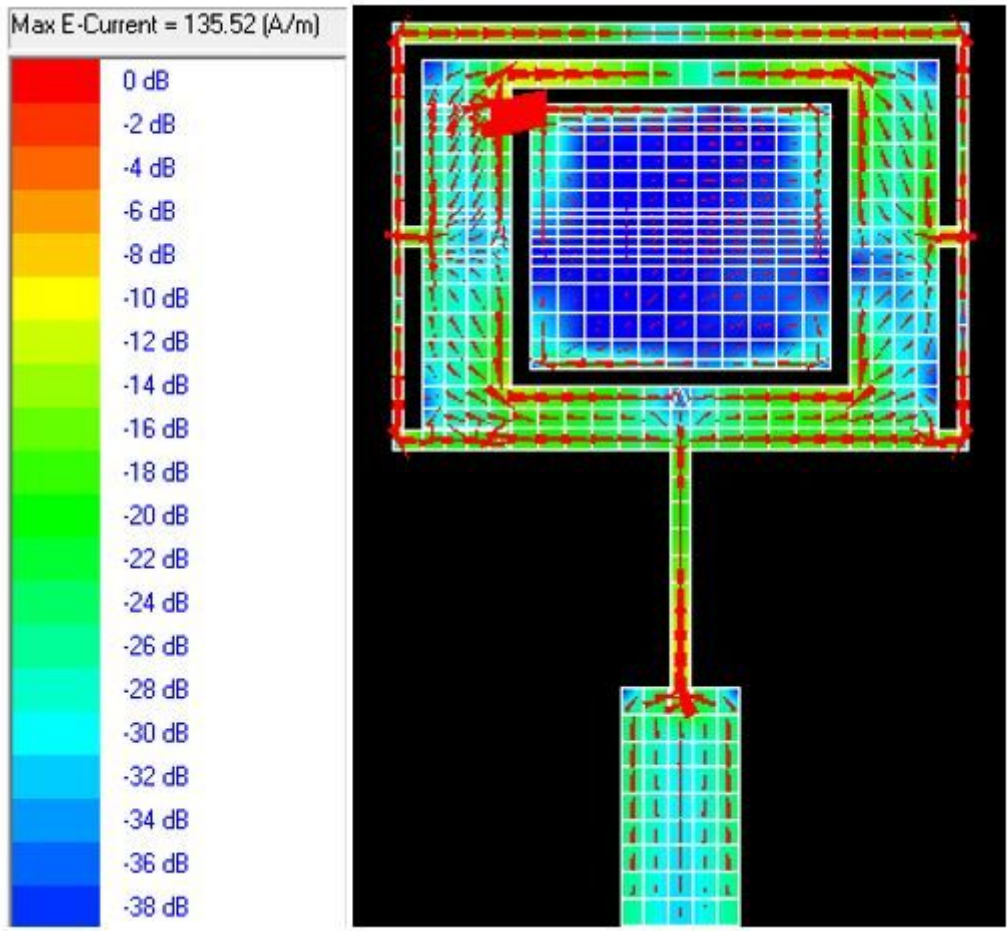


Figure 16

Current distribution of CCSR-SCS Antenna at 8.1 GHz

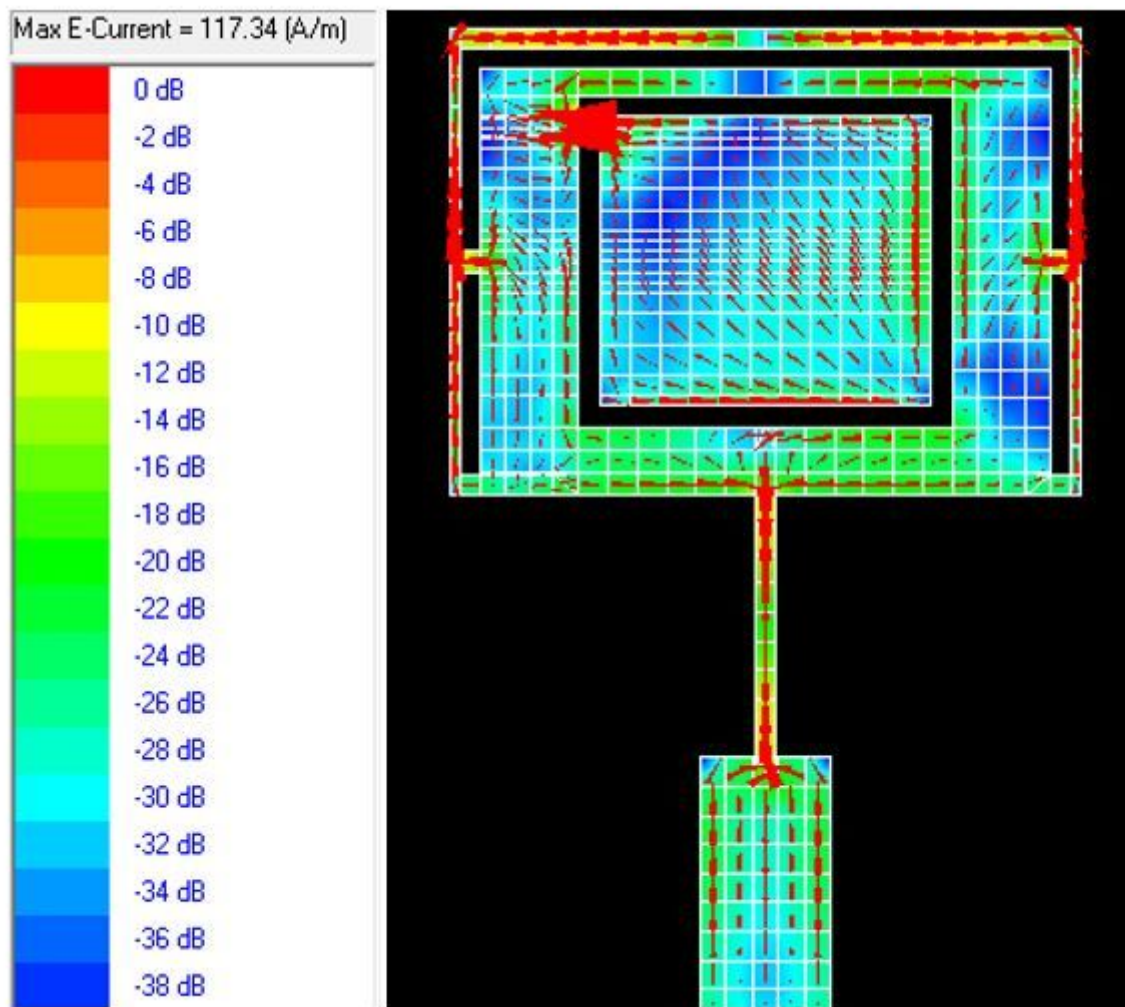


Figure 17

Current distribution of CCSR-SCS Antenna at 10.1 GHz